*Journal of The Electrochemical Society*, **153** (12) C814-C821 (2006)
0013-4651/2006/153(12)/C814/8/$20.00 © The Electrochemical Society

# Electrodeposited $Ni_{1-x}Co_x$ Nanocrystalline Thin Films

## Structure–Property Relationships

**D.-Y. Park,[a,*,z] K. S. Park,[a] J. M. Ko,[b] D.-H. Cho,[c] S. H. Lim,[c] W. Y. Kim,[d] B. Y. Yoo,[e] and N. V. Myung[e,*]**

[a]*Department of Applied Materials Engineering and* [b]*Department of Chemical Technology, Hanbat National University, Daejeon 305-719, Korea*
[c]*Department of Advanced Materials Science and Engineering, Kangwon National University, Chuncheon, Kangwon-do 200-701, Korea*
[d]*Advanced Materials Research and Development Center, Korea Institute of Industrial Technology, Incheon 406-130, Korea*
[e]*Department of Chemical and Environmental Engineering, University of California at Riverside, Riverside, California 92521, USA*

Electrodeposition of nanocrystalline Ni and $Ni_{1-x}Co_x$ thin films from chloride baths was systematically investigated by varying the electrodeposition parameters including electrolyte composition (i.e., $Co^{2+}$ ion concentration), additive (i.e., saccharin), solution pH, and current density. Their effects on the film growth mechanism, film composition, residual stress, microstructure, grain size, and surface morphology were studied. $Ni_{1-x}Co_x$ thin films electrodeposited from the baths without the addition of saccharin always showed tensile stress mode (145–367 MPa) with varying $Co^{2+}$ ion concentration, solution pH, and current density. In the presence of saccharin, the $Ni_{1-x}Co_x$ thin films showed either tensile stress or compressive stress mode, depending on the electrodeposition conditions. Especially, it was observed from a cross-sectional TEM observation that Ni thin film electrodeposited from the bath containing saccharin exhibited the formation of an amorphous Ni layer (about 300 nm thick) at the initial stage of the film growth. Also, $Ni_{1-x}Co_x$ thin films electrodeposited from the bath with/without the addition of saccharin showed the formation of the interface phase layer (about 10–110 nm thick), which has the chemical composition of 50 atom % Ni and 50 atom % Co.
 [DOI: 10.1149/1.2353792] 

Manuscript submitted March 7, 2006; revised manuscript received August 2, 2006. Available electronically October 9, 2006.

Electrodeposited Ni and $Ni_{1-x}Co_x$ thin films have been intensively studied because of their potential applications in microelectromechanical systems (MEMS),[1-3] LIGA,[4] electronic devices (e.g., spintronics, magnetic storages, optical recording devices, and integrated sensors),[5,6] and several other industries (e.g., automotive, manufacturing, and chemical process).[7] Ni and $Ni_{1-x}Co_x$ thin/thick films have been incorporated into magnetic-MEMS devices including sensors, microactuators, micromotors, and frictionless microgears because of their excellent physical properties.[1,3,4,8] Magnetic layer thickness in MEMS can range from a few nanometers to hundreds of micrometers, depending on the applications. Residual stress of the electrodeposited films is an important factor for incorporating magnetic materials in MEMS devices. High stress in magnetic thin/thick films may result in the malfunctioning of MEMS devices because of delamination of the deposited films from MEMS structures.

Numerous studies of the electrodeposited Ni thin/thick films have been carried out.[4,9-11] Typical nickel plating baths are chloride, sulfate, sulfamate, and mixed sulfate-chloride (i.e., Watts-type) baths.[11] When a sufficient amount of sulfur-containing additives such as benzoyl sulfamide (saccharin) or naphthalene trisulfonic acid (NTSA) is added to Ni plating baths, residual stress of Ni electrodeposits can be reduced to almost none. When added in greater quantities, these additives result in compressively stressed Ni deposits. Weil[12-14] reviewed various methods to measure residual stress of the electrodeposited films, the effects of electrodeposition parameters on residual stress in various pure metals (e.g., Cu, Ni, Co, and Zn), and the suggested hypotheses for the causes of residual stress in the electrodeposited films. Even though several hypotheses have been proposed to explain the causes of residual stress in the electrodeposited films, no overall hypothesis has been formulated to date. Dini[15] also reviewed residual stress in various electrodeposited materials. Ni electrodeposited from sulfamate baths exhibited the lowest stress value of 59 MPa compared to sulfate, chloride, bromide, and fluoroborate baths. Dini et al.[11] investigated the influence of sulfur on the properties of the electrodeposited Ni using a Charpy test and Knoop hardness test. They reported that the electrodeposited Ni film containing greater than 170 ppm sulfur was highly notch sensitive. Film hardness was shown to be a direct function of sulfur content.

Even though there are many studies on the electrodeposited $Ni_{1-x}Co_x$ thin films, they focused mostly on anomalous codeposition,[16-20] the applications of the magnetic $Ni_{1-x}Co_x$ materials in MEMS devices,[3] mechanical properties,[21] electrochemical properties,[22,23] or anion effects.[24] There is a lack of detailed studies correlating the electrodeposition parameter and the role of sulfur-containing additive (e.g., saccharin) with the property in the electrodeposited $Ni_{1-x}Co_x$ thin films. Especially, binary iron group alloys including NiCo, NiFe, and FeCo exhibit a so-called anomalous codeposition in which the less noble metal is deposited preferentially under certain conditions.[16-20] The mechanism of anomalous codeposition in iron group alloys was studied by several researchers. The behavior of anomalous codeposition may be attributed to an inhibition effect of the less noble metal on the more noble metal.

This paper is the extended research work of our previous result.[25] In this study, we investigated the effect of the electrodeposition parameters including metal ion concentration, solution pH, current density, and saccharin on film growth mechanism, residual stress, microstructure, grain size, and surface morphology of the electrodeposited Ni and $Ni_{1-x}Co_x$ thin films. Specifically, We studied the effect of an impurity element (sulfur) on the growth mechanism of Ni and $Ni_{1-x}Co_x$ thin films using a cross-sectional transmission electron microscopy (TEM) observation.

## Experimental

Ni and $Ni_{1-x}Co_x$ thin films were electrodeposited from chloride baths. Table I lists the plating solution composition investigated. NaCl and boric acid were used as supporting electrolyte and pH buffer, respectively. Solution was exposed to air and solution pH was adjusted with KOH or HC1. Ni and $Ni_{1-x}Co_x$ thin films were galvanostatically electrodeposited using an EG&G PAR potentiostat/galvanostat (model 263A or 273) at room temperature without stirring. The cathode current efficiency was deduced from differential mass measurement. The effects of the solution $Co^{2+}/Ni^{2+}$ ratio on the properties including film composition, current efficiency, residual stress, microstructure and surface morphology of $Ni_{1-x}Co_x$ films were studied by varying $Co^{2+}$ concentration

* Electrochemical Society Active Member.
z E-mail: dypark@hanbat.ac.kr

**Table I. Bath compositions and operating conditions (unless otherwise noted) for Ni and $Ni_{1-x}Co_x$ thin films electrodeposited from chloride baths (M = mol $dm^{-3}$).**

| Chemical/condition | Concentration (M) |
|---|---|
| $Ni^{2+}$ (as $NiCl_2 \cdot 6H_2O$) | 0.2 |
| $Co^{2+}$ (as $CoCl_2 \cdot 6H_2O$) | 0–0.206 |
| NaCl | 0.7 |
| $H_3BO_3$ | 0.4 |
| Saccharin | 0 or 0.01 |
| pH | 2–6 |
| Current density | 1–25 mA $cm^{-2}$ |
| Temperature | Room temperature (24°C) |

from 0.03 to 0.206 M, with 0.2 M $Ni^{2+}$ ion concentration, solution pH 4, and 10 mA $cm^{-2}$. The effects of solution pH on the properties of $Ni_{1-x}Co_x$ films were investigated by varying solution pH from 2 to 6, with 0.2 M $Ni^{2+}$ and 0.05 M $Co^{2+}$ ion concentrations, and 10 mA $cm^{-2}$. Also, the effects of current density (CD) on the properties of $Ni_{1-x}Co_x$ films were investigated by varying current density from 1 to 25 mA $cm^{-2}$, with 0.2 M $Ni^{2+}$ and 0.05 M $Co^{2+}$ ion concentrations, and solution pH 4. Ni and $Ni_{1-x}Co_x$ films were electrodeposited on Cu substrates (PN 1194, Specialty Testing & Development Co.); nickel sheet was used as a soluble anode. The residual stress of the $Ni_{1-x}Co_x$ films was measured by a deflection method with a deposit stress analyzer (model 683, Specialty Testing & Development Co.) and calculated by Stoney's equation.[15,26,27] Figure 1a shows a schematic of the apparatus for the electrodeposition of Ni and $Ni_{1-x}Co_x$ thin films to measure residual stress of the thin films. A Cu test strip (PN 1194, Specialty Testing & Development Co.) with a constant electrodeposited area of 7.74 $cm^2$ is located at the center of the storage tank (a total volume of 2.5 L). Figure 1b and c shows the dimension of the Cu test strip for measuring residual stress of the thin film. One side of the leg in the Cu test strip was laminated with polymer to prevent the electrodeposition of Ni or $Ni_{1-x}Co_x$ films. The other side (cross-hatched area) of the leg was not laminated with polymer to deposit the thin film. Electrodeposition of Ni or $Ni_{1-x}Co_x$ films was conducted without stirring of electrolyte. Stirring of electrolyte can affect the stress value because the Cu test strip is very thin (0.06 mm thick) and flexible. Cross-sectional TEM (model JEM-2010, JEOL, Ltd.) was used to characterize the microstructure of Ni and $Ni_{1-x}Co_x$ films. Structural information was obtained using electron diffraction and a bright-field image, operating at 200 kV. Samples for TEM observation were prepared by a conventional procedure, including mechanical polishing, dimpling, and Ar ion milling or focused ion beam milling (FIB). Surface morphology and film composition were examined using scanning electron microscopy (SEM) (model JSM-6300, JEOL, Ltd.) operating at 20 kV and the working distance of 17 mm, and energy-dispersive spectroscopy (EDS) (model ISIS, Oxford Instruments), respectively. An X-ray diffractometer (XRD) (model D/MAX 2500H, RIGAKU) with Cu Kα radiation (operating at 45 kV) was used for the identification of the phase and the measurement of the grain size in the thin films. The conditions of XRD were a scanning range of 30–100° with 0.03° increments and a 1 s collection time per increment.

## Results and Discussion

Figure 2 shows the cross-sectional TEM micrographs of Ni thin films electrodeposited with/without the addition of saccharin. In the presence of saccharin, an amorphous layer (approximately 300 nm thick) grows first on the Cu substrate at the beginning of electrodeposition and then the nanocrystalline Ni layer (or close to amorphous Ni) is electrodeposited (Fig. 2b) as shown in the bright-field image and the corresponding selected area diffraction pattern (SADP). The SADP clearly shows that the first layer from the Cu substrate is amorphous Ni and the second Ni layer nanocrystalline

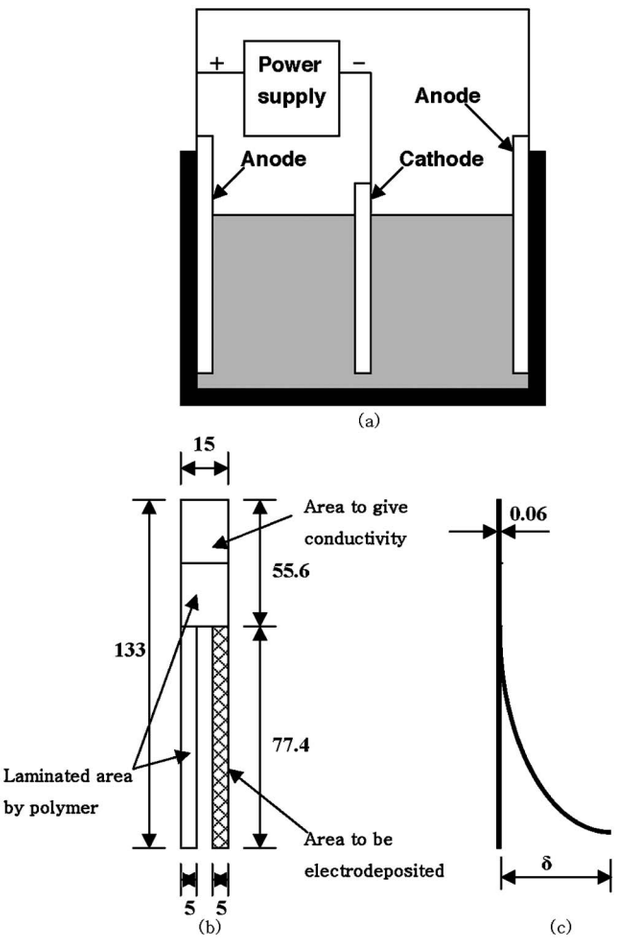


**Figure 1.** (a) Schematic of apparatus for electrodeposition, (b) dimensions of Cu test strip for measuring residual stress of thin film, cross-hatched area is electrodeposited by Ni or CoNi, and (c) deflection of Cu test strip after electrodeposition (δ: relative displacement). Unit: mm.

Ni (or close to amorphous Ni). In the absence of saccharin, the formation of the amorphous layer at the early stage of electrodeposition was not observed (Fig. 2a). The amount of sulfur from EDS analysis was measured to be about 1 atom % in Ni thin film electrodeposited from the bath containing 0.01 M saccharin. It is believed that the impurity element of sulfur from the source of saccharin influenced the film growth mechanism in Ni thin film. Figures 3 and 4 show the cross-sectional TEM micrographs of $Ni_{1-x}Co_x$ thin films electrodeposited with/without the addition of saccharin. The $Ni_{1-x}Co_x$ thin films were electrodeposited from the bath containing 0.2 M $NiCl_2$ and 0.05 M $CoCl_2$ at 10 mA $cm^{-2}$, pH 4.0, and room temperature without stirring. The deposit thickness of $Ni_{1-x}Co_x$ thin films was measured to be about 2.7 μm from the cross-sectional TEM micrographs. The $Ni_{1-x}Co_x$ thin film electrodeposited without the addition of saccharin (Fig. 3) exhibits the formation of a thicker and continuous interface phase layer (about 110 nm thick) at the beginning of the film growth along the interface between the Cu substrate and $Ni_{1-x}Co_x$ thin films. The chemical composition of the interface phase layer (point A in Fig. 3a) was measured to be 49 atom % Ni and 51 atom % Co from EDS analysis as shown in Fig. 5. The chemical composition of the remaining film (point B, C, and D in Fig. 3a) in $Ni_{1-x}Co_x$ thin film was 71 atom % Ni and 29 atom % Co shown in Fig. 6. EDS analysis for the remaining film was conducted from the near interface phase layer to the top of the remaining film at three different positions [the position near the

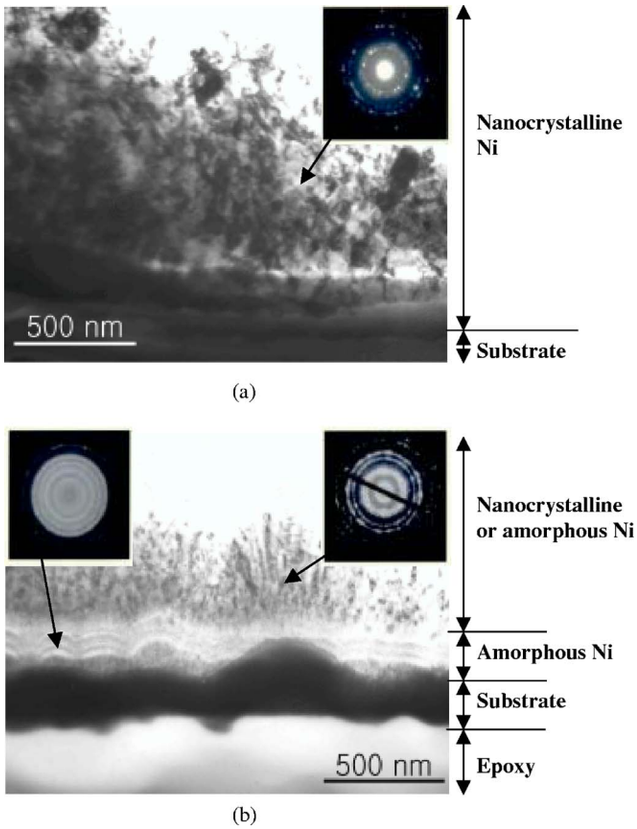


**Figure 2.** Cross-sectional TEM bright field images and SAD patterns of Ni thin films electrodeposited with/without saccharin: (a) no saccharin and (b) 0.01 M saccharin. Deposit thickness approximately 3 μm.

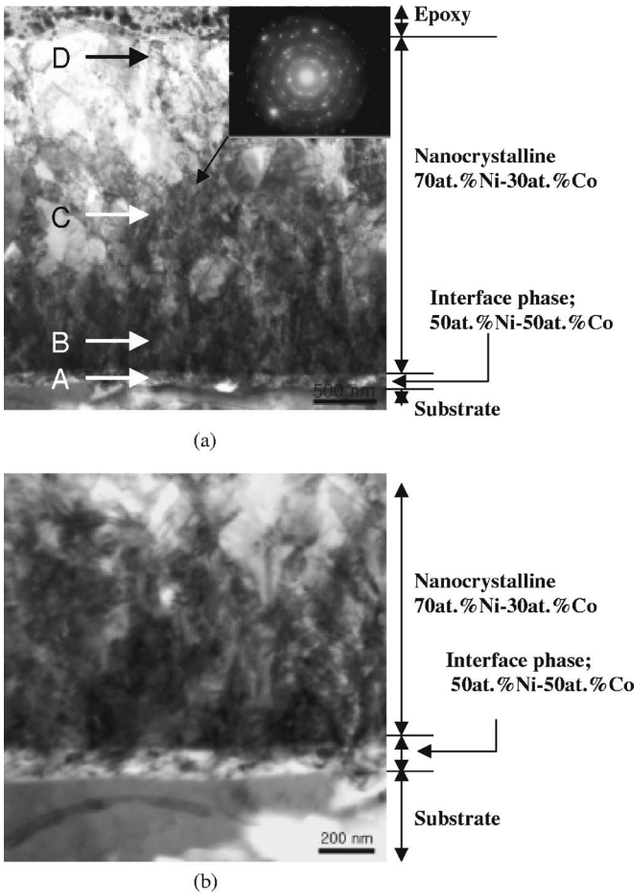


**Figure 3.** Cross-sectional TEM bright-field images and SAD pattern of $Ni_{1-x}Co_x$ thin films electrodeposited without saccharin: (a) low magnification and (b) high magnification. Deposit thickness approximately 3 μm.

interface phase (Fig. 6a), the intermediate position (Fig. 6b), and the near top surface position (Fig. 6c) of the remaining film] to check on any compositional differences between the remaining film. The chemical compositions were measured to be nearly same at the three different areas. The peak of the chemical element Fe in EDS analysis resulted from the Cu substrate itself. The amount of Fe element was found to be higher at the area near to the Cu substrate compared to the top surface area. Fe was not detected at the near top surface position (point D in Fig. 3a) of the $Ni_{1-x}Co_x$ thin films, as shown in Fig. 6c. Figure 4 shows that the $Ni_{1-x}Co_x$ thin films electrodeposited with the addition of saccharin also exhibited a thinner and discontinuous interface phase layer (less than 20 nm thick). The chemical composition of the remaining film was also measured to be 70 atom % Ni and 30 atom % Co from EDS analysis. Therefore, it is evident that the addition of element Co in Ni thin film results in the formation of the interface phase layer, which consists of 50 atom % Ni and 50 atom % Co, at the early stage of electrodeposition. The addition of saccharin in $Ni_{1-x}Co_x$ thin films results in the formation of a thinner and discontinuous interface phase layer. SAD patterns from the interface phase layer could not be taken because the aperture size in TEM compared to thickness of the interface phase layer is too large to get SAD patterns. Further investigation to reveal the exact growth mechanism at the beginning stage of electrodeposition in Ni and $Ni_{1-x}Co_x$ thin films is needed.

Figure 7 shows the change in the film compositions as a function of solution pH, and current density in the electrolyte solution and in the presence or absence of saccharin. Figure 7a shows that the deposit Ni and Co contents with/without saccharin are independent of solution pH. The $Ni^{2+}/Co^{2+}$ ratio on the electrodeposited $Ni_{1-x}Co_x$ thin films was independent of the addition of saccharin. However, the deposit Ni content increased from 28 to 78 atom % with increasing current density from 1 to 25 mA $cm^{-2}$; the deposit Co content decreased from 72 to 22 atom %, as shown in Fig. 7b. Current density strongly influenced the $Ni^{2+}/Co^{2+}$ ratio on the electrodeposited $Ni_{1-x}Co_x$ thin films, but the $Ni^{2+}/Co^{2+}$ ratio was independent of the addition of saccharin. Zech et al.[18-20] experimentally and theoretically studied anomalous codeposition of iron group alloys. They reported that Ni deposition was inhibited by codeposition of Co. They suggested that inhibition or enhancement of the deposition rate is attributed to interactions between codepositing species. Therefore, the higher Co content (72–60 atom % at low current density (1 to 3 mA $cm^{-2}$) in $Ni_{1-x}Co_x$ thin films electrodeposited from the baths with/without the addition of saccharin may result from the inhibition of Ni by codeposition of Co. From our previous paper,[25] the deposited Co content increased from 23 to 85 atom % with increasing $Co^{2+}$ ion concentration in the plating baths from 0.03 to 0.206 M. The $Ni^{2+}/Co^{2+}$ ratio on the electrodeposited $Ni_{1-x}Co_x$ thin films was nearly identical in the absence or presence of saccharin. Deposited sulfur content in $Ni_{1-x}Co_x$ thin films electrodeposited from the baths containing 0.01 M saccharin were measured to be less than 1 atom % and was independent of $Co^{2+}$ ion concentration. The detection limit of EDS for chemical elements may be about 1%. The sulfur amount of less than 1 atom % in this study is very small and may be in the range of detection limit. However, if we consider the effect of sulfur on film stress, microstructure, and growth mechanism in $Ni_{1-x}Co_x$ thin film, the small amount of sulfur is not negligible.

Figure 8 shows the dependence of current efficiency on $Co^{2+}$ ion concentration (Fig. 8a), solution pH (Fig. 8b), and current density

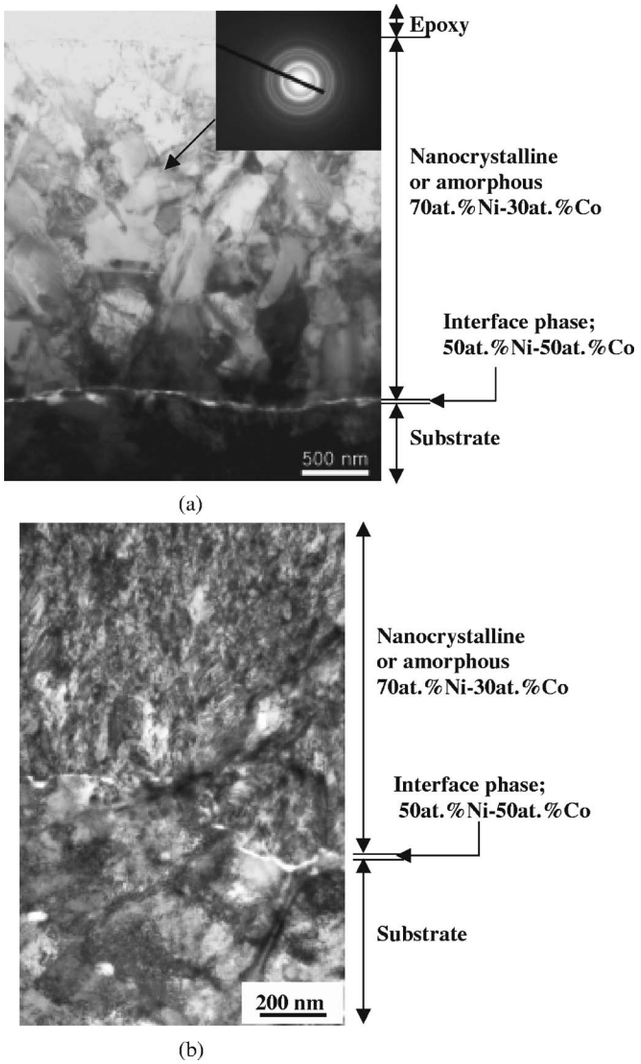


**Figure 4.** Cross-sectional TEM bright-field images and SAD pattern of $Ni_{1-x}Co_x$ thin films electrodeposited with 0.01 M saccharin: (a) low magnification and (b) high magnification. Deposit thickness approximately 3 μm.

(Fig. 8c) in Ni and $Ni_{1-x}Co_x$ thin films. Current efficiency of more than about 90% was almost independent of $Co^{2+}$ ion concentration, whereas current efficiency slightly increased with increasing solution pH and slightly decreased with increasing current density. From the cross-sectional TEM analysis in this study, it was also observed

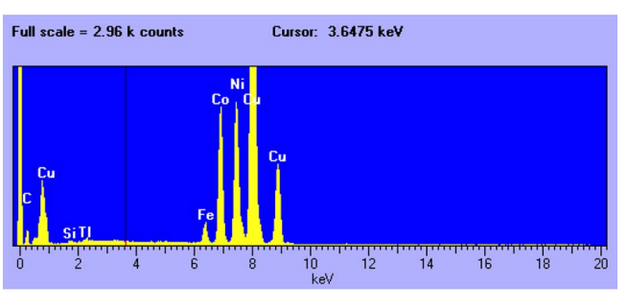


**Figure 5.** (Color online) EDS spectra showing chemical composition of the interface phase layer (point A in Fig. 3a) in $Ni_{1-x}Co_x$ thin films electrodeposited without saccharin; 49 atom % Ni–51 atom % Co.

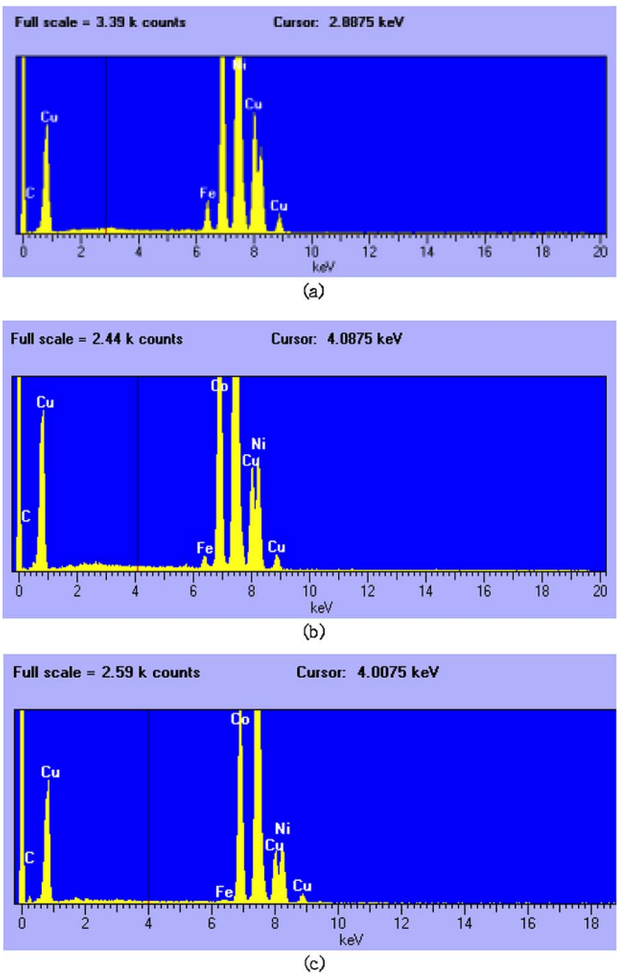


**Figure 6.** (Color online) EDS spectra showing the same chemical composition (71 atom % Ni–29 atom % Co) of nanocrystalline $Ni_{1-x}Co_x$ thin films electrodeposited without saccharin at (a) near interface phase (point B in Fig. 3a), (b) intermediate area (point C in Fig. 3a), and (c) near top surface area (point D in Fig. 3a).

that about 2.7 μm thick films were obtained despite using the deposition time for obtaining 3 μm thick films, as shown in Fig. 3a and 4a. There is good agreement between the current efficiency and the deposit film thickness in this study. Fenineche et al.[21] reported that the high current efficiency (93%) in CoNi electrodeposits from chloride baths was obtained at room temperature, pH 3.5, and current densities from 10 to 15 mA $cm^{-2}$. High current efficiency of more than 90% in this study appears to be in good agreement with the reported value (93%) by Fenineche et al.[21] Golodnitsky et al.[22] studied NiCo alloy electrodeposited from a sulfamate electrolyte with different anion additives. They observed an increase in the current efficiency from 65 to 82%, with increasing current density from 2 to 100 mA/$cm^2$. Solution pH and operating temperature were kept at 3 and 55°C, respectively. Therefore, it is believed that electrodeposition conditions including anion type, current density, and operating temperature strongly influenced the current efficiency.

Figure 9 shows the change of residual stress in electrodeposited $Ni_{1-x}Co_x$ alloys as a function of solution pH and current density in the plating solution with/without the addition of saccharin. Residual stresses of $Ni_{1-x}Co_x$ thin films with/without the addition of saccharin show a minimum at solution pH 4 (Fig. 9a). Unfortunately, previous data of solution pH effect on residual stress in $Ni_{1-x}Co_x$ thin films is not available for comparison. Weil[13] has summarized that there is a

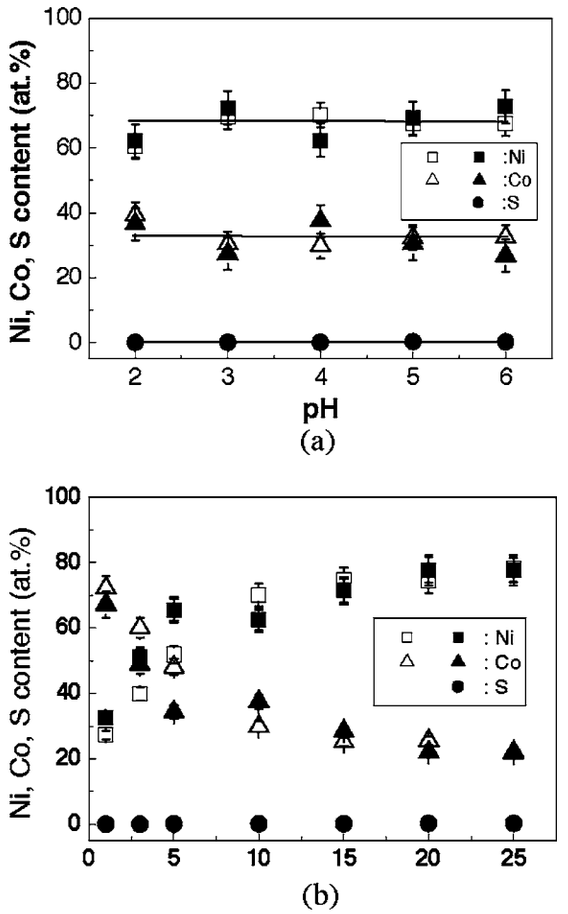


**Figure 7.** Dependence of film composition on solution pH and current density in $Ni_{1-x}Co_x$ thin films: (△, □) no saccharin and (■, ▲, ●) 0.01 M saccharin. Deposit thickness about 3 μm.

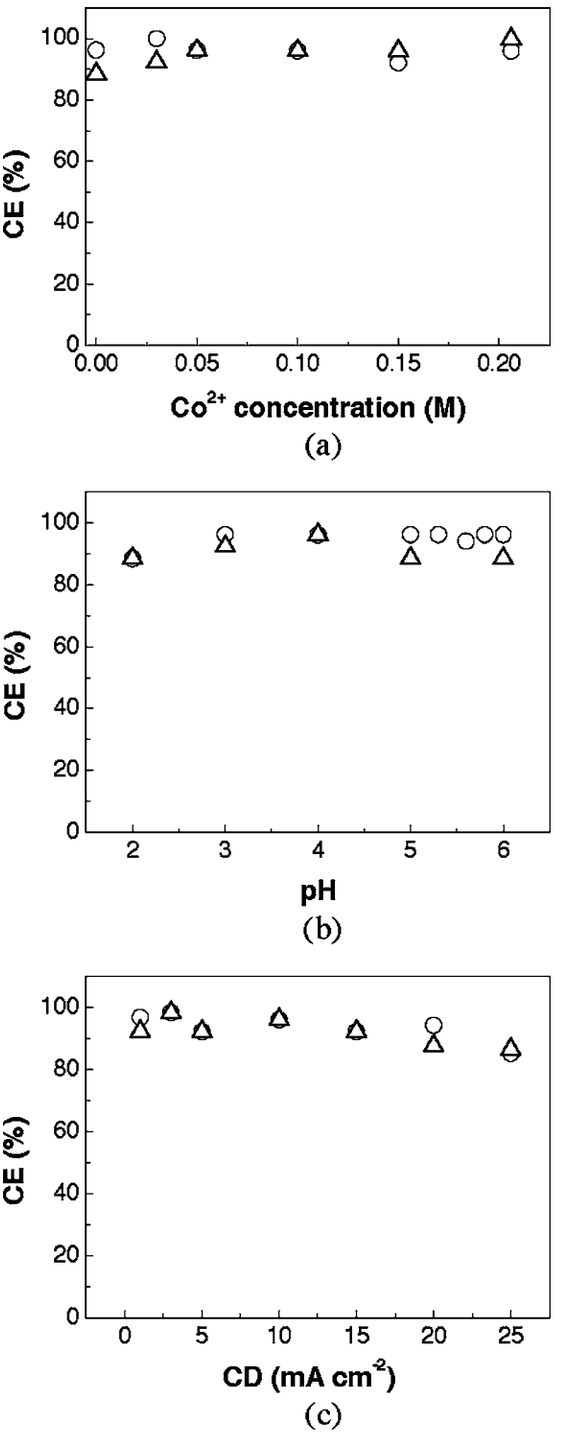


**Figure 8.** Dependence of current efficiencies in $Ni_{1-x}Co_x$ thin films on (a) $Co^{2+}$ ion concentration, (b) solution pH, and (c) current density; (○) no saccharin and (△) 0.01 M saccharin. Deposit thickness about 3 μm.

sharp rise of residual stress in Ni deposits in the range of solution pH values from 4 to 6. The exact value of solution pH where the stress begins to increase appears to depend greatly on plating conditions and the bath compositions. $Ni_{1-x}Co_x$ thin films in this study exhibited a little higher value of residual stress above solution pH 5. Residual stress of $Ni_{1-x}Co_x$ film from saccharin-free electrolytes was independent of current density (approximately 220 MPa) at low current density (1–10 mA $cm^{-2}$). However, $Ni_{1-x}Co_x$ films from saccharin-free electrolytes exhibited higher residual stress values of approximately 360 MPa at 15 and 20 mA $cm^{-2}$. $Ni_{1-x}Co_x$ electrodeposits from the baths containing 0.01 M saccharin show minimum residual stress of approximately 0 MPa at 10 mA $cm^{-2}$ (Fig. 9b). From our previous paper,[25] we replotted the stress changes in Ni and $Ni_{1-x}Co_x$ thin films as a function of deposit Co content (Fig. 9c). Residual stress of 145 MPa (tensile stress mode) was obtained in Ni thin film electrodeposited from saccharin-free electrolyte. Ni thin film deposited from saccharin-containing electrolyte exhibited a compressive stress mode (−85 MPa). It has been reported that Ni electrodeposited from additive-free Watts baths exhibits tensile stresses of 125–185 MPa.[28] Kushner[29] reported tensile stress values of 59–228 MPa from the baths with various different anions. They reported that the residual stress of Ni electrodeposited from chloride bath was measured to be 228 MPa. The difference between the reported value of residual stress (228 MPa) and that of this study (145 MPa) may be attributed to the different substrate and electrodeposition conditions, including $Ni^{2+}$ ion concentration and current density. It was suggested that codeposition of elemental sulfur in Ni electrodeposited from the bath with sulfur-containing organic additives results in the transition of residual stress from tensile to compressive mode.[13,28] As deposited Co content in $Ni_{1-x}Co_x$ thin films increased up to about 89 atom % in the absence of saccharin, residual stress of $Ni_{1-x}Co_x$ thin films increased from 173 to 262 MPa. $Ni_{1-x}Co_x$ thin films electrodeposited from the baths containing saccharin exhibited a transition from compressive

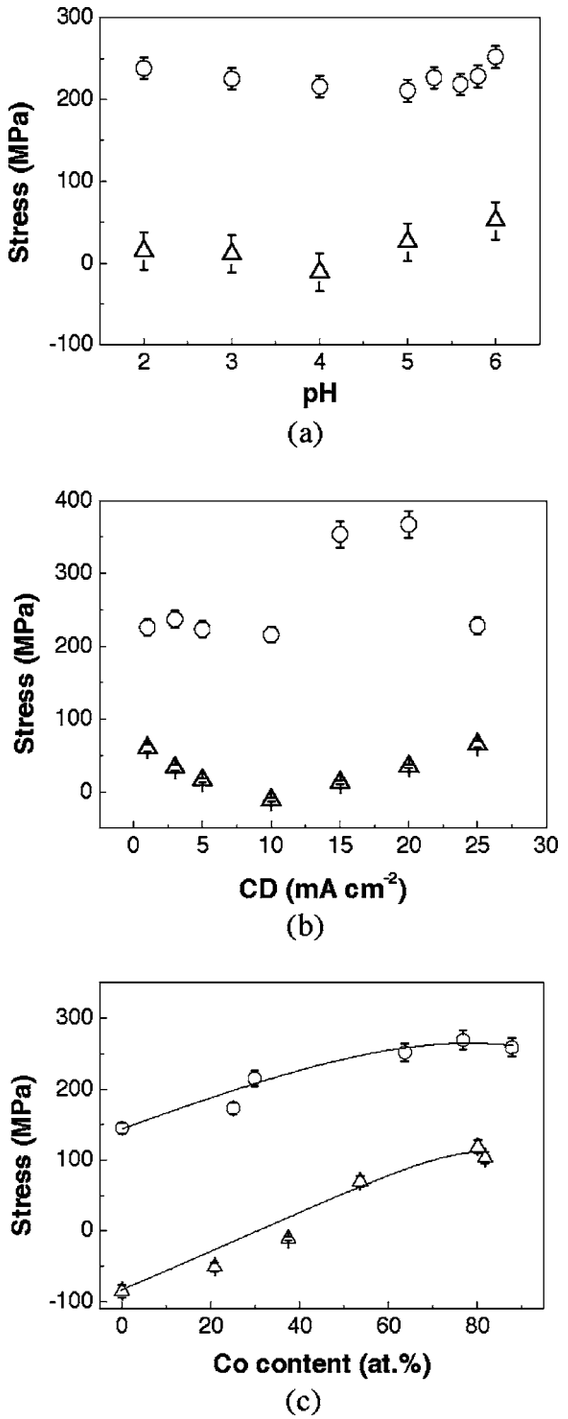


**Figure 9.** Dependence of residual stress in $Ni_{1-x}Co_x$ thin films electrodeposited from chloride baths on (a) solution pH, (b) current density, and (c) deposit Co content; (○) no saccharin and (△) 0.01 M saccharin. Deposit thickness approximately 3 μm.

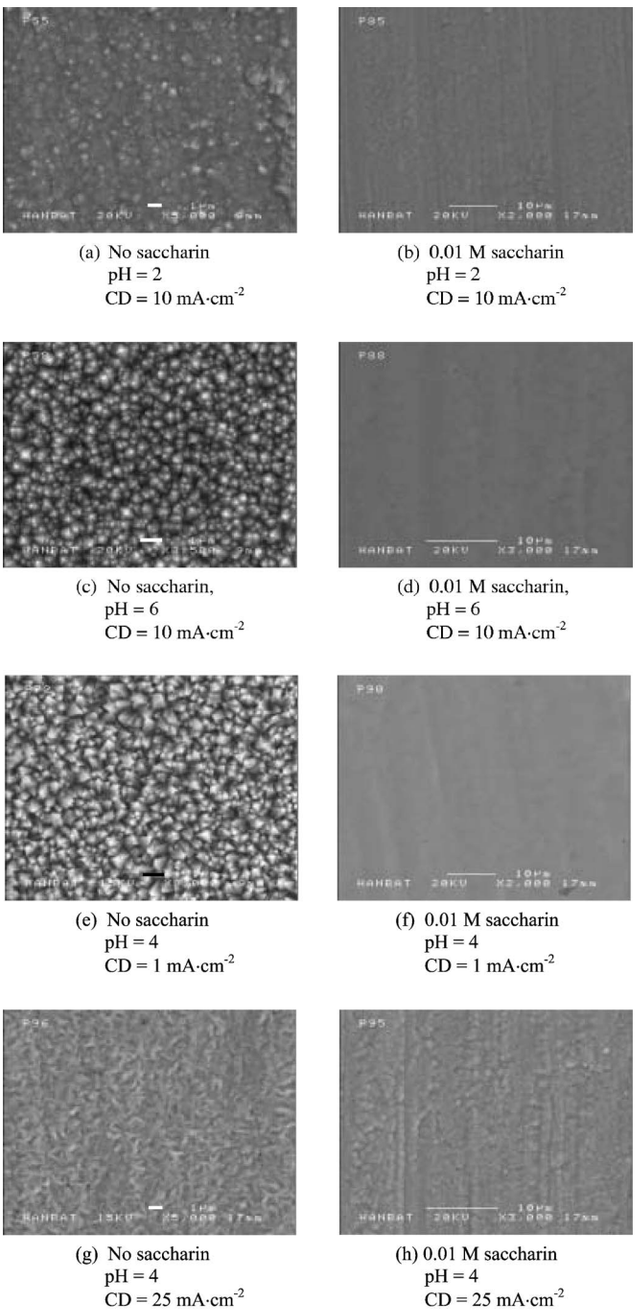


**Figure 10.** Dependence of surface morphology in $Ni_{1-x}Co_x$ thin films on solution pH and current density with/without saccharin. Deposit thickness approximately 3 μm.

(−51 MPa) to tensile stress mode (120 MPa). Almost zero-stress $Ni_{1-x}Co_x$ thin film was obtained at Co deposit content of 30–40 atom %. Small quantities (0.01–0.1 g/L) of most sulfur-containing additives in the plating bath rapidly reduce residual stress in Ni deposits.[15] It is well known that the saccharin as a source of sulfur effectively decreases the residual stress in Ni deposits.[13] The addition of saccharin lowers residual stress in Co deposits, but not as effectively as in Ni deposits. Thus, it can be hypothesized that the transition of residual stress from compressive to tensile stress mode in $Ni_{1-x}Co_x$ deposits with increasing $Co^{2+}$ ion concentration may be attributed to the lesser effect of sulfur in Co-rich deposits.

Figure 10 shows the dependence of surface morphology in $Ni_{1-x}Co_x$ thin films with/without saccharin on solution pH (Fig. 10a-d), and current density (Fig. 10e-h). It is evident that the addition of 0.01 M saccharin in $Ni_{1-x}Co_x$ plating baths strongly influenced the surface morphology. The $Ni_{1-x}Co_x$ thin films, which consist of about 35 atom % Co and about 65 atom % Ni in the absence of saccharin, exhibited a nodular surface morphology (Fig. 10a and c) with increasing solution pH from 2 to 6. In the presence of sac-

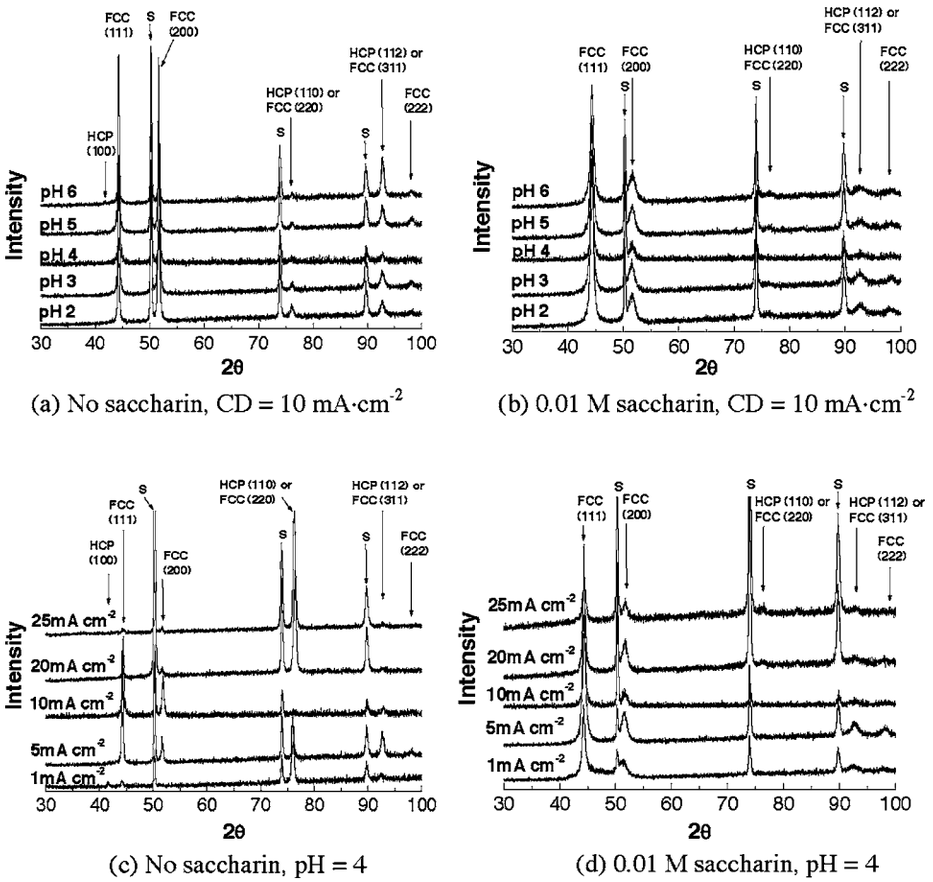


**Figure 11.** XRD patterns of $Ni_{1-x}Co_x$ thin films electrodeposited from plating bath with/without saccharin as a function of solution pH, and current density. $Ni^{2+}$: 0.2 M, $Co^{2+}$: 0.05 M. Deposit thickness approximately 3 μm (S: substrate).

charin, the $Ni_{1-x}Co_x$ thin films showed the smooth surface morphology (Fig. 10b and d). At low current density of 1 mA/cm$^2$, the $Ni_{1-x}Co_x$ thin film that consists of about 75 atom % Co and about 25 atom % Ni exhibited a pyramidal surface morphology (Fig. 10e). At high current density, the $Ni_{1-x}Co_x$thin film that consists of about 20 atom % Co and about 80 atom % Ni showed a nodular surface morphology (Fig. 10g).

Figure 11 shows the dependence of the XRD patterns in $Ni_{1-x}Co_x$ thin films with/without the addition of saccharin on solution pH (Fig. 11a and b), and current density (Fig. 11c and d). The XRD patterns of $Ni_{1-x}Co_x$ thin films electrodeposited from saccharin-free electrolyte consist of face-centered cubic (fcc) (111), fcc (200), fcc (220) [or hexagonal close-packed (hcp) (110)], fcc(311) [or hcp (112)], and fcc (222) at solution pH 2–6, as shown in Fig. 11a. $Ni_{1-x}Co_x$ thin films deposited from the baths containing 0.0.1 M saccharin (Fig. 11b) exhibited a similar microstructure with different intensity compared to $Ni_{1-x}Co_x$ thin films electrodeposited from saccharin-free electrolyte in Fig. 11a. $Ni_{1-x}Co_x$ thin films electrodeposited from saccharin-free electrolyte exhibited mixed hcp and fcc phases at 1 mA cm$^{-2}$; fcc (220) or hcp (110) is a dominant phase. The dominant phases in $Ni_{1-x}Co_x$ thin film electrodeposited at 5 and 10 mA cm$^{-2}$ are fcc (111) and fcc (200). The dominant phases are changed to be fcc (220) or hcp (110) at 20 and 25 mA cm$^{-2}$. The dominant phases are fcc (111) and fcc (200) in $Ni_{1-x}Co_x$ thin films deposited from the baths containing 0.01 M saccharin. There was not found any trend in microstructure with increasing current density. In the presence of saccharin, the line broadening of the XRD peaks of the dominant phases [fcc (111), fcc (200), and hcp (112) or fcc (311)] was clearly observed. The average grain sizes of fcc (111) and fcc (200) in $Ni_{1-x}Co_x$ thin films (Fig. 11a) electrodeposited from saccharin-free electrolyte were measured to be 55 and 48 nm, respectively. The grain size was calculated from the Scherrer formula. The average grain sizes of fcc (111) and fcc (200) in $Ni_{1-x}Co_x$ thin films (Fig. 11b) electrodeposited from the baths containing 0.01 M saccharin were measured to be 29 and 16 nm, respectively. The average grain sizes of fcc (111) and fcc (200) in $Ni_{1-x}Co_x$ thin films (Fig. 11c) electrodeposited from saccharin-free electrolyte were measured to be 49 and 44 nm, respectively. Also, the average grain sizes of fcc (111) and fcc (200) in $Ni_{1-x}Co_x$ thin films (Fig. 11d) electrodeposited from the baths containing 0.01 M saccharin were measured to be 32 and 16 nm, respectively. Therefore, it is evident that the addition of saccharin strongly influenced the grain size of the dominant phases. There exists a good agreement in grain refinement due to the addition of saccharin in Ni and $Ni_{1-x}Co_x$ thin films from XRD analysis and SAD patterns (Fig. 2b and Fig. 4a) in TEM. It was suggested that the stress difference between $Ni_{1-x}Co_x$ thin films with and without 0.01 M saccharin may result from the addition of saccharin in the plating baths (as a source of impurity element, sulfur) rather than the microstructure.[25] The amount of sulfur from EDS analysis was measured to be less than 1 atom % in Ni and $Ni_{1-x}Co_x$ thin films electrodeposited from the bath containing 0.01 M saccharin. The thin films deposited by physical or chemical vapor deposition or electrodeposition exhibit the residual stress, resulting in cracking or peeling the film.[30] If the pure thin film was deposited at high temperature and operated at lower temperature, the residual stress in thin film may be attributed to a mismatch in the coefficient of thermal expansion between the substrate and the film. If the pure thin film was deposited on a substrate under stress, the residual stress may result from a mismatch in the elastic modulus. It was also suggested that impurities and defects influence the residual stress of the thin film during deposition or solid-state transformation.[30,31] The thin film containing residual gas, oxygen, and water vapor usually exhibit compressive stress mode.[32,33] Therefore, it could be summa-

rized that the purer the film, the greater the tendency for tension, and oxygen and other impurities tend to give rise to compressive stress mode.[34]

## Conclusion

Residual stresses of $Ni_{1-x}Co_x$ thin films were strongly influenced by current density and $Co^{2+}$ ion concentrations. Solution pH slightly affected residual stress. The addition of saccharin in the Ni plating bath resulted in the changes of film growth mechanism, residual stress, surface morphology, grain size, and microstructure. The addition of saccharin in Ni thin film resulted in the formation of an amorphous Ni layer about 300 nm thick at the initial stage of film growth. The continuous interface phase layer (110 nm thick) which has different composition of 50 atom % Ni and 50 atom % Co was formed in $Ni_{1-x}Co_x$ thin films at the initial stage of film growth. The addition of saccharin in $Ni_{1-x}Co_x$ thin films resulted in not only the decrease of the thickness of the interface phase layer (from 110 to 50 nm) but also the formation of a discontinuous interface phase layer (less than 20 nm thick). For saccharin-free electrolyte, Ni thin film showed tensile stress mode (145 MPa). However, Ni thin film electrodeposited from the bath containing 0.01 M saccharin exhibited compressive stress mode (−85 MPa). The transition of residual stress from compressive to tensile stress mode in $Ni_{1-x}Co_x$ thin films electrodeposited from the baths containing 0.01 M saccharin was observed with increasing $Co^{2+}$ ion concentrations. It was suggested that the effect of saccharin (as a source of an impurity element, sulfur) on residual stress was less effective in Co-rich thin films compared to Ni-rich thin films. Therefore, Co-rich thin films show a tensile stress mode despite the addition of saccharin in the plating bath.

## Acknowledgments

This work was supported by grant no. R01-2003-000-10597-0 from the Basic Research Program of the Korea Science & Engineering Foundation. B.Y.Y. and N.V.M. acknowledge funding support from the American Electroplaters and Surface Finishers (AESF), project no. 115.

*Hanbat National University assisted in meeting the publication costs of this article.*

## References

1. J. W. Judy and R. S. Muller, *J. Microelectromech. Syst.*, **6**, 249 (1997).
2. K. Kataoka, S. Kawamura, T. Itoh, K. Ishikawa, H. Honma, and T. Suga, *Sens. Actuators, A*, **103**, 116 (2003).
3. H. H. Yang, N. V. Myung, J. Yee, D.-Y. Park, B.-Y. Yoo, M. Schwartz, K. Nobe, and J. W. Judy, *Sens. Actuators, A*, **97-98**, 88 (2002).
4. S. M. Allameh, J. Lou, F. Kavishe, T. Buchheit, and W. O. Soboyejo, *Mater. Sci. Eng., A*, **371**, 256 (2004).
5. F. Czerwinski, A. Zielinska-Lipiec, and J. A. Szpunar, *Acta Mater.*, **47**, 2553 (1999).
6. C. A. Moina and M. Vazdar, *Electrochem. Commun.*, **3**, 159 (2001).
7. C.-C. Hu, C.-Y. Lin, and T.-C. Wen, *Mater. Chem. Phys.*, **44**, 233 (1996).
8. J. W. Judy, R. S. Muller, and H. H. Zappe, *J. Microelectromech. Syst.*, **4**, 162 (1995).
9. W. M. Yin, S. H. Whang, and R. A. Mirshams, *Acta Mater.*, **53**, 383 (2005).
10. K. P. Larsen, A. A. Rasmussen, J. T. Ravnkilde, M. Ginnerup, and O. Hansen, *Sens. Actuators, A*, **103**, 156 (2003).
11. J. W. Dini, H. R. Johnson, and H. J. Saxton, *J. Vac. Sci. Technol.*, **12**, 766 (1975).
12. R. Weil, *Plating*, **57**, 1231 (1970).
13. R. Weil, *Plating*, **58**, 50 (1971).
14. R. Weil, *Plating*, **58**, 137 (1971).
15. J. W. Dini, *Electrodeposition-The Materials Science of Coatings and Substrates*, Chap. 9, Noyes Publications, Park Ridge, NJ (1993).
16. S. Hessami and C. W. Tobias, *J. Electrochem. Soc.*, **136**, 3611 (1989).
17. K. Y. Sasaki and J. B. Talbot, *J. Electrochem. Soc.*, **142**, 775 (1995).
18. N. Zech, E. J. Podlaha, and D. Landolt, *J. Appl. Electrochem.*, **28**, 1251 (1998).
19. N. Zech, E. J. Podlaha, and D. Landolt, *J. Electrochem. Soc.*, **146**, 2886 (1999).
20. N. Zech, E. J. Podlaha, and D. Landolt, *J. Electrochem. Soc.*, **146**, 2892 (1999).
21. N. Fenineche, C. Coddet, and A. Saida, *Surf. Coat. Technol.*, **41**, 75 (1990).
22. D. Golodnitsky, N. V. Gudin, and G. A. Volyanuk, *J. Electrochem. Soc.*, **147**, 4156 (2000).
23. A. Bai and C.-C. Hu, *Electrochim. Acta*, **47**, 3447 (2002).
24. D. Golodnitsky, Yu. Rosenberg, and A. Ulus, *Electrochim. Acta*, **47**, 2707 (2002).
25. D.-Y. Park, R. Y. Song, J. M. Ko, B. Y. Yoo, and N. V. Myung, *Electrochem. Solid-State Lett.*, **8**, C23 (2005).
26. B.-Z. Lee and D. N. Lee, *Acta Mater.*, **46**, 3701 (1998).
27. *Electronic Thin Film Science for Electrical Engineers and Materials Scientists*, K.-N. Tu, J. W. Mayer, and L. C. Feldman, Editors, Chap. 4, Macmillan Publishing Company, New York (1992).
28. *Modern Electroplating*, 4th ed., G. A. Di Bari, M. Schlesinger, and M. Paunovic, Editors, pp. 139–199, Wiley-Interscience, New York (2000).
29. J. B. Kushner, *Met. Finish.*, **56**, 81 (1958).
30. F. A. Smidt, *Int. Mater. Rev.*, **35**, 61 (1990).
31. W. Esinger, *Rev. Sci. Instrum.*, **63**, 5217 (1992).
32. H. Leplan, J. Y. Robic, and Y. Pauleau, *J. Appl. Phys.*, **79**, 6926 (1996).
33. H. Leplan, B. Geenen, and J. Y. Robic, *J. Appl. Phys.*, **78**, 962 (1995).
34. S. Tamulevičius, *Vacuum*, **51**, 127 (1998).